Are microseismic ground displacements a significant geomorphic agent?

Matthew J. Brain[1], Nicholas J. Rosser, Emma C. Norman and David N. Petley

Department of Geography, Durham University, Science Site, South Road, Durham, DH1 3LE, UK

Abstract

This paper considers the role that microseismic ground displacements may play in fracturing rock via cyclic loading and subcritical crack growth. Using a coastal rock cliff as a case study, we firstly undertake a literature review to define the spatial locations that may be prone to microseismic damage. It is suggested that microseismic weakening of rock can only occur in 'damage accumulation zones' of limited spatial extent. Stress concentrations resulting from cliff height, slope angle and surface morphology may nucleate and propagate a sufficiently dense population of microcracks that can then be exploited by microseismic cyclic loading. We subsequently examine a 32-day microseismic dataset obtained from a coastal cliff-top location at Staithes, UK. The dataset demonstrates that microseismic ground displacements display low peak amplitudes that are punctuated by periods of greater displacement during storm conditions. Microseismic displacements generally display limited preferential directivity, though we observe rarely occurring sustained ground motions with a cliff-normal component during storm events. High magnitude displacements and infrequently experienced ground motion directions may be more damaging than the more frequently occurring, reduced magnitude displacements characteristic of periods of relative quiescence. As high magnitude, low frequency events exceed and then increase the damage threshold, these extremes may also render intervening, reduced magnitude microseismic displacements ineffective in terms of damage accumulation as a result of crack tip blunting and the

generation of residual compressive stresses that close microcracks. We contend that damage resulting from microseismic ground motion may be episodic, rather than being continuous and in (quasi-)proportional and cumulative response to environmental forcing. A conceptual model is proposed that describes when and where microseismic ground motions can operate effectively. We hypothesise that there are significant spatial and temporal limitations on effective microseismic damage accumulation, such that the net efficacy of microseismic ground motions in preparing rock for fracture, and hence in enhancing erosion, may be considerably lower than previously suggested in locations where high magnitude displacements punctuate 'standard' displacement conditions. Determining and measuring the exact effects of microseismic ground displacement on damage accumulation and as a trigger to macro-scale fracture in the field is not currently possible, though our model remains consistent with field observations and conceptual models of controls on rockfall activity.

Keywords: rock slope; microseismicity; displacement; strain; stress; damage; rockfall

1. Introduction and scope

Microseismic monitoring techniques have recently been used to detect and characterise a range of geomorphic processes, including ocean wave energy delivery to coastal cliffs (Adams et al., 2002; Young et al., 2011; 2012 ; Dickson and Pentney, 2012), river bedload transport (Hsu et al., 2011; Tsai et al., 2012), glacier fracture and hydrology (Roux et al., 2008; West et al., 2010) and rock sliding and avalanching (Deparis et al., 2008; Dammeier et al., 2011). Whilst microseismicity has been used in these studies as a remote proxy for process, Adams et al. (2005) hypothesised that microseismic ground motions may themselves constitute a significant yet largely unrecognised geomorphic process that is worthy of further attention.

Adams et al. (2005) reported an exponential decay in the magnitude of micron-scale (0.1 – 1 × 10^1 μm) displacements along a transect perpendicular to the face of a coastal rock cliff at Monterey Bay, California, USA. By comparison with ocean wave data, Adams et al. (2005) demonstrated that the observed flexure results from the loading of the foreshore platform by water waves, notably longer-period incident sea swell ocean waves (10 – 20 s period). Similar observations were also made by Young et al. (2011; 2012) at infragravity frequencies (20 – 170 s period). Adams et al. (2005) suggested that the low magnitude (micron-scale) cyclic nature of cliff-top microseismic ground displacements may be sufficient to damage the rock mass via a fatigue process, such that overall rock mass strength is progressively reduced as microcracks propagate, interact and coalesce (Attewell and Farmer, 1973; Main et al., 1993). If microseismic ground motions are significant in reducing rock mass strength, macro-scale rock fracture could therefore occur at ambient deviatoric stresses that are considerably less than the peak strength values of intact (undamaged) rocks (Sunamura, 1992; Xiao et al., 2011). Under this model, by creating planes of weakness, microseismic fatigue could play a key role in governing the timing and distribution of landform and landscape susceptibility to change (cf. Allison, 1996; Molnar et al., 2007; Moore et al., 2009; Dühnforth et al., 2010; Clarke and Burbank 2010; 2011; Koons et al., 2012). If microseismic cyclic loading is effective in weakening rocks in an incremental, preparatory manner and, hence, permitting fracture to occur more readily, this may be an important yet rarely considered process in driving slope failure.

As a preparatory geomorphic process (cf. Gunzberger et al., 2005), microseismic cyclic loading theoretically relies on an extremely high number of effective (damaging) load cycles to exert any significant geomorphic consequence, since the damage increment resulting from each loading cycle is likely to be exceedingly small, yet not cumulatively negligible (Adams

et al., 2005). For this to occur to a degree sufficient to be comparable to other damage-inducing processes, the spatial and temporal opportunity for microseismic damage must be sufficiently extensive. As such, the Adams et al. (2005) microseismic damage model is based on two critical assumptions, as follows:

1. the spatial extent of the 'damage accumulation zone' is sufficiently large and continuous that the low magnitude strains have sufficient opportunity to operate for a period of time sufficient to cause significant damage to rock. The exact spatial extent of the damage accumulation zone was not physically or theoretically constrained by Adams et al. (2005), but was suggested to be of the order of tens of metres inland from the cliff face. As such, ongoing microseismic strains were implicitly assumed to be able to cause damage at any location within the damage accumulation zone, to a degree commensurate with the magnitude of strain resulting from microseismic cliff flexure;
2. all microseismic ground displacements resulting from ocean wave loading of the foreshore platform create incremental rock-damaging strains. The magnitude of damage resulting from each load cycle was deemed to be a function of the magnitude of strain and the existing damage condition of the rock mass relative to its pristine state. Damage (weakening) was assumed to be cumulative and ongoing, increasing with the number of loading cycles experienced by the rock and, hence, through time.

We address these assumptions to provide an alternative interpretation of the potential effectiveness of microseismic ground motions in accumulating damage in rock and to reconsider the microseismic damage model proposed by Adams et al. (2005). We firstly present an alternative assessment of how and where microseismic ground motions are likely to act as an effective geomorphological process in brittle materials. Secondly, a 32-day record

of microseismic displacements recorded in a rocky coastal cliff environment is analysed to consider the key characteristics of the observed microseismic displacements to explore the possible temporal evolution of rock strength in response to microseismic loading. Thirdly, a conceptual model of the spatial and temporal occurrence or rock-damaging microseismic ground motions is developed. Finally, we explore the implications of the model and consider its potential validity using previously published datasets on rockfall activity in rocky coastal cliffs.

2. Defining the damage accumulation zone

2.1 Microseismic strain and stress magnitudes

Subcritical brittle microfracture and fatigue crack growth caused by cyclic loading have been shown to damage and weaken rocks in laboratory studies under compressive and tensile loading conditions (Attewell and Farmer, 1973; Lavrov et al., 2002; Erarslan and Williams, 2012a). Such laboratory studies report results from tests that employ a variety of dynamic loading frequencies, including those comparable with the longer-period ground motions observed in coastal cliffs by Adams et al. (2005) and Young et al. (2011) (cf. Attewell and Farmer, 1973; Tien et al., 1990; Li et al., 1992). Attewell and Farmer (1973) concluded that the lowest frequencies tested (0.1 Hz; 10 s period) caused failure in fewer cycles than those of the same stress amplitude but higher frequency ($\leq$ 20 Hz; 0.05 s period), suggesting that ground motions resulting from foreshore wave loading, comparable to those observed by Adams et al. (2005) and Young et al. (2011) are potentially, in relative terms, highly damaging and conducive to fatigue crack growth.

Adams et al. (2005) and Young et al. (2012) estimated strains (dimensionless) resulting from microseismic ground motions of the order 0.1 to 1×10^{-6}. These estimated strain values are

many orders of magnitude lower than the peak strain values of rocks under monotonic loading (Young et al., 2012). For example, for a variety of rock types tested in unconfined compression, such peak strain values are in the range 0.5 - 2 × 10^{-2} (e.g. Heap et al., 2010).

Prior to failure, microseismic displacement and, hence, strain (ε, i.e. relative displacement and deformation within the cliff-forming material) result in a (quasi-)proportional application of a stress (σ) to the rock mass, following Hooke's law:

$$\sigma = E\varepsilon \quad (1)$$

where E is Young's modulus of elasticity. Applied microseismic stresses (σ_{min} and σ_{max}) act relative to the mean (in situ static) stress (σ_{mean}). Calculated and reported dynamic stresses resulting from microseismic loading are of the order 1 to 10 × 10^{-3} MPa (Adams et al., 2005; Young et al., 2012), assuming E = 20 GPa. Peak unconfined compressive strength values (UCS) can range from 40 MPa (Bentheim Sandstone; Heap et al., 2009) to 360 MPa (Icelandic basalt; Vinciguerra et al., 2005). Rocks tend to be weaker under tensile loading conditions and peak tensile strength values can range from 4 MPa (Ellington Mudstone) to 70 MPa (Cefn Coed Sandstone) (Hobbs, 1964). Stresses resulting from cliff flexure may therefore represent a greater proportion of peak (failure) stress under tensile baseline conditions.

2.2 Brittle microfracture and subcritical crack growth

Whilst stresses and strains induced by microseismic ground motions are a small fraction of peak values observed under monotonic loading, localised brittle microfracture damage can occur in rock at stresses significantly less than peak strength (Scholz, 1968; Martin and Chandler, 1994; Mitchell and Faulkner, 2008). The macro-scale mechanical behaviour of

rock in the brittle domain is dependent on rock microstructure (Potyondy, 2007), notably the presence, density and interaction of microcracks (Tapponier and Brace, 1976; Eberhardt et al., 1999). The remotely applied microseismic stresses are not necessarily transmitted equally throughout the rock mass (Potyondy, 2007). Stress magnitudes can be locally modified within the rock mass at sites of stress concentration, such as pore spaces, grain or crystal boundaries, microscopic flaws and petrological structures (Cai et al., 2004), allowing microcrack nucleation as stresses exceed local strength (Kranz, 1983). The magnitude of the elastic stress field at the microcrack tip is described by K, the stress intensity factor (cf. Janssen et al., 2002, for example), defined as:

$$K = \sigma\sqrt{\pi a} \quad (2)$$

where σ is the remotely applied stress and a is the microcrack length. Equation (2) describes a an isolated two-dimensional crack in an infinite space, which we use for simplicity but note that alternative terms are required for microcracks of differing geometry (cf. Brady and Brown, 2004). Increasing K values results in an increase in the potential for microcrack growth (Janssen et al., 2002).

When populations of microcracks are sufficiently dense to permit interaction at a critical scale, crack coalescence results, ultimately culminating in macro-scale fracture (Bieniawski, 1967; Martin and Chandler, 1994; Main et al., 1993). The process of microcrack propagation and coalescence can result in measurable and continuous pre-failure macro-scale strains that culminate in slope failure or rockfall activity at the field scale (Petley et al., 2005a, b; Rosser et al., 2007; Stock et al., 2011).

2.3 Damage thresholds and cyclic stress amplitudes

There are key differences between laboratory dynamic loading tests and microseismic loading conditions experienced and observed in the field. The stress amplitudes reproduced in strain-controlled tests under laboratory conditions are significantly greater than those that result from microseismic displacements observed by Adams et al. (2005) and Young et al. (2011; 2012). For example, the cyclic stress amplitude range used by Attewell and Farmer (1973) increased the maximum dynamic compressive stress to between 40 and 75 % of the UCS (57 to 130 MPa) of the dolomite samples used; mean compressive stresses were between 25 % and 50 % of the UCS. Similarly, dynamic stresses applied to Belgian 'blue' limestone by Lavrov et al. (2002) were between 50 and 70 % of the peak Brazilian tensile strength observed. These high stress amplitudes employed in dynamic laboratory tests were sufficient to nucleate microcracks. The level of stress required to initiate microcracking is described by the staged brittle failure model conceptualised and developed by Brace et al. (1966), Bieniawski (1967) and Martin and Chandler (1994) (Fig. 1 a), which we use as a conceptual basis on the assumption that similar thresholds are observed under tensile and shear loading conditions (see Lavrov et al., 2002; Jafari et al., 2003). In a typical strain-controlled monotonic compression test, the microcracking process is characterised by five key stages:

1. Crack closure, as pre-existing and microcracks favourably oriented to the applied load close. The stress-strain curve is non-linear, displaying an increase in stiffness;
2. Linear elastic deformation, which occurs when the majority of microcracks have closed at σ_{cc}, the crack closure stress threshold;
3. Crack initiation and stable crack growth occur as the stress level for crack initiation, σ_{ci}, is exceeded. σ_{ci} occurs at approximately 30 – 50 % of the peak strength, σ_{fs} (Brace et al., 1966; Eberhardt et al, 1999). Microcracks grow in the direction of the major principal

stress, σ_1 (Hoek and Bieniawski, 1965; Lajtai, 1971; Peng and Johnson, 1972). In the stable crack growth stage under monotonic loading, removal of the applied load can stop crack growth, or limit the rate of growth (Eberhardt et al., 1999);

4. Crack damage and unstable crack growth occur as stress levels exceed the crack damage threshold, σ_{cd}. This point may be evident as a clear reduction in stiffness on the stress-strain curve (Fig. 1 a) and results from microcrack coalescence and an accelerating crack growth rate that cannot be halted by removing the applied stress (Bieniawski, 1967). σ_{cd} occurs between 70 and 90 % of σ_{fs} (Bieniawski, 1967); and
5. Failure at σ_f followed by post peak behaviour, which in fully fractured brittle materials may not be present.

Eberhardt et al. (1999) demonstrated that characteristic normalised axial strains exist for each of the microcracking thresholds under compressive loading conditions. Crack initiation occurs at approximately 45 % of the peak strain at failure and crack damage and propagation occurs at strains greater than approximately 68 % of the peak failure strain (Eberhardt et al., 1999).

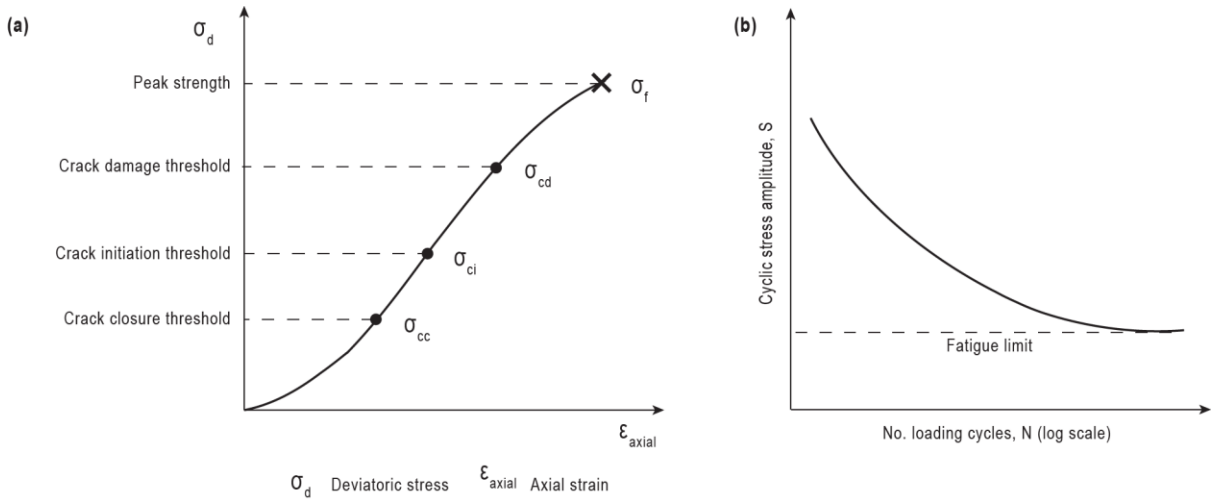

200

201 Fig. 1. (a) Stress-strain curve showing the stages of crack development (adapted from
202 Eberhardt et al., 1999) (b) Typical S-N curve for materials showing a fatigue limit.

Critical stress and strain levels have previously been emphasised in field and modelling studies. Exceedance of the crack initiation threshold, σ_{ci}, creates a sufficiently dense population of microcracks that can subsequently be exploited by 'environmental' forces (Rosser et al., 2007), such as variations in pore water pressure (Petley et al., 2005a, b; Ng and Petley, 2009), ambient temperature (Gischig et al., 2011a, b) and/or potentially ocean wave impact loads (Adams et al., 2002). These processes cause further accumulation of damage resulting from, for example, time-dependent creep and fatigue processes driven by subcritical crack growth (Rosser et al., 2007). In turn, this can cause stress redistribution and further microcrack damage in a progressive failure process (Terzaghi, 1962; Bjerrum, 1967; Eberhardt et al., 2004), causing the crack damage threshold, σ_{cd}, to be exceeded, triggering a transition from secondary to tertiary creep and, ultimately, rupture (Petley et al., 2005a, b).

Importantly, critical stress and strain levels are required to nucleate microcracks before fatigue processes can exert an influence on microcrack densities and rock strength. Such critical stressing is achieved in the high cyclic stress amplitude laboratory tests undertaken by Attewell and Farmer (1973), for example. However, where σ_{mean} does not exceed σ_{ci}, small fluctuations in the stress field generated by microseismic ground displacements are highly unlikely to be of sufficient magnitude to increase the stress state to a level that can induce crack initiation and unstable crack growth.

The importance of stress amplitude in causing failure in materials subjected to dynamic loading can also be demonstrated by plotting stress amplitude, S, against number of cycles to failure, N (logarithmic scale), to produce S-N curves (Fig. 1 b). Each point used to define the curve reflects a single specimen that has been subjected to constant amplitude loading until failure. Critically, however, not all stress amplitudes result in failure, as demonstrated by the

plateau in the S-N curve. There is a threshold stress amplitude, the fatigue limit (σ_f). Cyclic stress amplitudes less than σ_f do not result in growth of fatigue cracks and, hence, rocks can be subjected to an infinite number of stress cycles at this stress amplitude (Janssen et al., 2002). Full characterisation of fatigue strength requires S-N curves to be obtained for all mean stress conditions and for compressive, tensile and shear stresses (cf. Attewell and Farmer, 1973; Jafari et al., 2003; Lavrov et al., 2002; Erarslan and Williams, 2012a). Greater mean stress values result in a decreasing resistance to smaller amplitude loads (Suresh, 1998). This effect is likely to be significant when mean deviatoric stress is greater than the σ_{ci}, resulting in a microfracture population that is prone to fatigue crack growth during cyclic loading (Attewell and Farmer, 1973).

2.4 Loading direction

The existence of the crack closure stage in the microcrack development model described above suggests that the direction of stress application relative to pre-existing flaws may be important during cyclic loading, particularly in rocks displaying marked micro-structural anisotropy (e.g. Nasseri et al., 2010). However, the directional component of microseismic cyclic loading is currently poorly constrained and the effects of variability in loading direction are not explicitly considered in the microseismic damage model of Adams et al. (2005).

2.5 Fatigue damage accumulation zones

The discussion presented above suggests that microseismic ground motions require intact rocks to have experienced a critical level of stress and strain (i.e. a pre-damaged condition) before they can propagate microfractures and accelerate their growth. Critical stressing reduces the value of the fatigue limit, σ_f, allowing low cyclic stress amplitudes generated by

249 microseismic ground motions to cause fatigue crack growth. In order to define the nature of
250 fatigue damage accumulation zones, it is necessary to consider where such critical stressing
251 occurs in geomorphic systems. We can speculate with reasonable confidence on the basis of
252 published results and theory, but it is emphasised that we cannot yet exactly define the level
253 of critical stressing and the associated value (or range of values) of σ_f required to permit the
254 microseismic stresses generated in a geomorphic setting to be effective in causing fatigue.

255 In the context of a coastal rock cliff, or indeed any rock slope, stress distributions are
256 controlled by cliff height and local (near-cliff face) stress concentrations that result from
257 slope angle, cliff face geometry and the presence and nature of asperities at a variety of
258 spatial scales (Jafari et al., 2003; Wolters and Müller, 2008; Young and Ashford, 2008;
259 Wyllie and Mah, 2010; Gischig et al., 2011a, b; Stock et al., 2011; Styles et al., 2011).
260 Modelling work by Wolters and Müller (2008) suggested that shear stresses along (potential)
261 slip surfaces reduce significantly in the first few metres from the cliff face, suggesting that
262 the critical stressing necessary to form microcracks and, hence, increase susceptibility to
263 cyclic damage processes is more likely to have been achieved close to the cliff face and so
264 microseismic fatigue may be more effective here. Styles et al. (2011) demonstrated how
265 critical levels of stress propagate along a spatially concentrated failure surface that is
266 relatively close to the cliff face (10^0 to 10^1 m). In both of these modelling studies, deviatoric
267 stress and resultant strain are shown to quickly reduce to lower levels with perpendicular
268 distance from the fracture surface. The same distance-decay effect in stress and damage away
269 from the fracture surface has previously been reported in major tectonic fault zones (Anders
270 and Wiltschko, 1994; Moore and Lockner, 1995; Vermilye and Scholz, 1998; Janssen et al.,
271 2001; Wilson et al., 2003; Faulkner et al., 2006). Such observed exponential decreases in

microcrack density have been interpreted to reflect the stress gradient away from the fracture (fault) (Mitchell and Faulkner, 2008).

A strong spatial pattern in the effectiveness of microseismic ground motions in propagating and connecting microcrack populations results from this spatial pattern of in situ stresses. The critical levels of stress and strain (i.e. exceedance of the crack initiation threshold as a minimum) required to reduce the fatigue limit to a level that can be exploited by microseismic ground displacements only occur in spatially restricted circumstances. Rock that is not within a critically-stressed fatigue damage accumulation zone surrounding pre-formed and incipient fractures may therefore be considered unlikely to undergo microseismic fatigue damage.

3. Magnitude and frequency of rock-damaging microseismic ground displacements

3.1 Study site

The study site is a section of the coastline on the North York Moors National Park in northeast England located approximately 1.5 km to the east of the village of Staithes (Fig. 2). This section of coastline has been previously been studied by Agar (1960), Robinson (1974), Lim et al. (2010; 2011), Rosser et al. (2007), Barlow et al. (2012), Norman (2012) and Norman et al. (in revision), providing a baseline dataset on cliff erosion rates, patterns of rockfall activity and energy delivery to coastal cliffs.

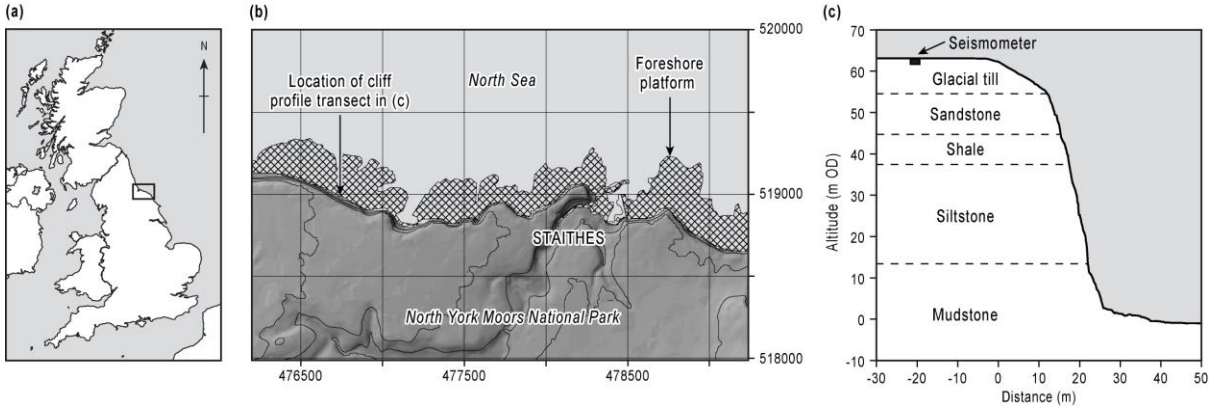

290

291 Fig. 2. (a) Map of the United Kingdom showing the approximate location of the North
292 Yorkshire coastline (boxed area). (b) Study site location on the coast of the North York
293 Moors National Park. Hatched area denotes the foreshore platform. 25 m topographic
294 contours are from Ordnance Survey PlanForm data (under license from EDINA, 2010). (c)
295 Cross-section of the coastal cliff study site at Boulby obtained using Terrestrial Laser
296 Scanning (see Rosser et al., 2007 and references therein) displaying seismometer installation
297 location and schematic display of cliff lithology.

298 The cliffs at our study site are oriented approximately 290˚ to c. 110˚, generating exposure to
299 easterly and northerly North Sea storm events, but shelter from prevailing southwesterly
300 weather systems.

301 The c. 70 m high, near-vertical cliffs at the site are cut into the interbedded mudstones,
302 shales, siltstones, ironstones and sandstones of the Lower Jurassic Redcar Mudstone and
303 Staithes Sandstone formations (Rawson and Wright, 2000), which dip at 2˚ to the southeast
304 and are capped by approximately 10 m of overconsolidated Devensian glacial till.

305 The site has a tidal range of c. 6 m. This submerges the base of the cliff (approximately 1.6
306 m above Ordnance Datum – approximately mean sea level) during high spring tides. The
307 cliffs are fringed by a foreshore platform that extends approximately > 200 m seaward (Fig.
308 2) and is fully exposed when high atmospheric pressure systems coincide with lowest
309 astronomical tides. Beach deposits are generally absent. Wave fetch at the site is limited in
310 most directions by the boundary coasts of the North Sea. In turn, this controls and limits the
311 wave periods that can develop. The Cefas WaveNet wave buoy located approximately ~18
312 km to the northwest of the site recorded a mean wave period of approximately 5 s and a
313 model value of 3 – 4 s between July 2008 and July 2010 (Norman, 2012).

314 3.2 Methods

315 3.2.1 Microseismic data

316 Ground motions were measured using a Güralp 6TD broadband seismometer, which has a flat
317 frequency response range 0.033 to 100 Hz (period response range of 30 to 0.01 s). We
318 monitored velocity (m/s) in three axes (vertical, z; north-south, n; and east-west, e) at a
319 sampling rate of 100 Hz (Nyquist frequency of 50 Hz). The seismometer location is displayed
320 in Fig. 2. Further details on seismometer installation, data collection and quality screening to

check for and remove any anthropogenic noise or earthquakes signals are provided by Norman (2012) and Norman et al. (in revision). Notably, a considerable section of microseismic data that is ostensibly not related to the local and/or regional signals of interested here has been removed from 15 July 2009 (Fig. 3 a).

Ground tilt causes a component of the vertical gravitational acceleration to be recorded in the horizontal acceleration channels (Rodgers, 1968). Whilst tilt 'contamination' of the vertical component is generally considered minimal (Graizer, 2006), recorded horizontal (e and n) acceleration (and hence velocity and displacement) can be overestimated unless corrected for (Young et al., 2012). The effects of ground tilt on horizontal displacement increase with increasing period (Webb and Crawford, 1999; Crawford and Webb, 2000) but have been shown to be minimal at frequencies less than 0.14 Hz (~7 s period) (Young et al., 2012). To avoid the effects of tilt on our displacement data, we consider the frequency band 0.14 – 1 Hz (1 – 7 s period). In addition, we refer to horizontal (e and n) displacements as 'apparent' to signify that no tilt corrections have been applied. To obtain the selected frequency band, we applied a bandpass filter to the output velocity data for each component of ground motion (z, n and e). We subsequently integrated the filtered velocity data with trapezoidal accuracy to obtain time-series of displacement data (μm), which retain the same sampling frequency (100 Hz) of the original velocity data.

As described above, the 1 – 7 s period band contains both the mean and model wave periods recorded offshore. Norman et al. (in revision) demonstrated a landward decay in the vertical energy signal recorded at additional seismometers placed in a cross-shore transect for 1, 2 and 5 s period ground motions at the site. Since the microseismic signals recorded are not uniform at all seismometers, such signals are deemed to be above background levels. In

addition, the cross-shore decay in energy signal suggests a similar cliff flexure and strain signal that results from foreshore loading by incident swell waves, as observed at other sites (cf. Adams et al., 2005; Young et al., 2011; 2012). Hence, the 1 – 7 s period band is appropriate for our study on the assumption that the displacements recorded at our seismometer are observed at greater magnitude closer to the cliff edge and decay in magnitude with distance inland.

Results are presented from two 16-day periods: 2 to 17 July 2009; and 27 November to 12 December 2009. These were selected to represent typical 'summer' and 'winter' conditions on the North Yorkshire coastline.

3.2.2 Meteorological, hydrographic and oceanographic data

Prevailing weather data (rainfall, atmospheric pressure, wind direction and wind velocity), collected at five-minute intervals, were obtained from the UK Meteorological Office monitoring station Loftus, 1.5 km west of the site.

Tidal (predicted tidal height and observed tidal residual) data were obtained for Whitby, approximately 15 km to the southeast of Staithes, from the British Oceanographic Data Centre, and oceanographic (significant wave height and peak wave period) from a wave buoy ~18 km offshore. Time series plots of meteorological, tidal, oceanographic and microseismic displacement data for the July 2009 and November/December 2009 monitoring periods are displayed in Fig. 3 (a and b, respectively).

These datasets are used to consider general 'environmental' conditions in the region and, hence, at our study site. We do not consider the modifying effects of nearshore bathymetry on

365 oceanographic and hydrographic conditions here; further analysis of such effects is provided
366 in Norman et al. (in revision).

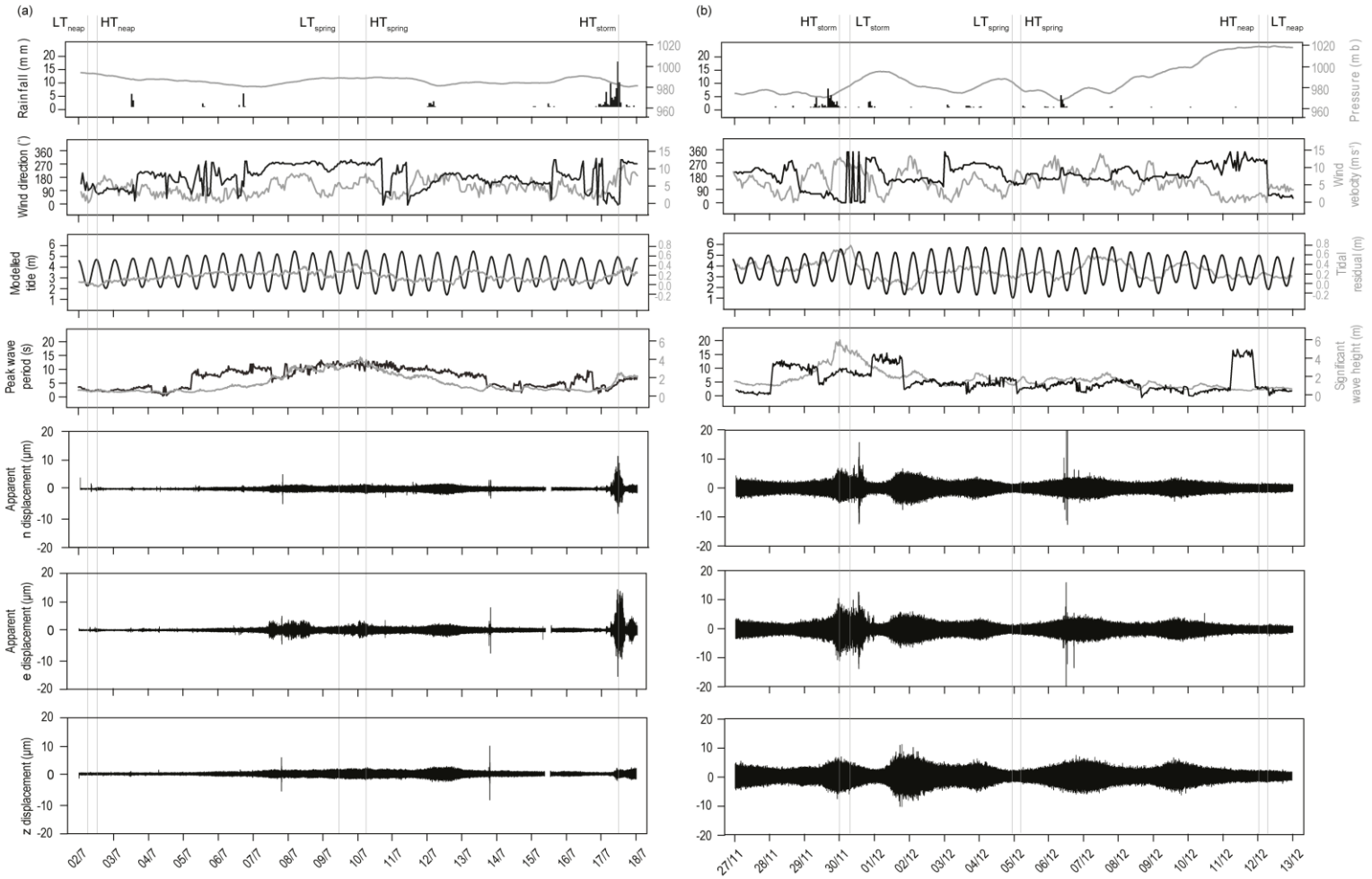

367

368 Fig. 3. Time series plots of meteorological, tidal, oceanographic and microseismic data for (a) July 2009 monitoring period and (b) November-
369 December 2009 monitoring period. Vertical grey lines indicate the centre-point of characteristic displacement scenarios discussed in the text.
370 Black datasets correspond to left-hand vertical axes. Grey datasets correspond to right-hand vertical axes. Gap in seismic data on 15 July 2009
371 reflects manual removal of ground motions not explained by local conditions, in accordance with Adams et al. (2005) and Young et al. (2012).
372 See main text for an explanation of notation.

373 3.3 Microseismic data

374 3.3.1 General patterns and controls on displacement magnitude

375 Cliff ground motion responds to both proximal and distal loading, and can be broadly
376 correlated with marine and weather conditions (Norman, 2012; Norman et al., in revision). In
377 both July 2009 (Fig. 3 a), microseismic ground displacements generally exhibit low
378 amplitudes that range from approximately –1 μm to 1 μm in z, n and e directions, punctuated
379 by periods of greater displacement. In November/December 2009, 'background'
380 displacements are marginally greater, ranging from -2 μm to 2 μm, but a similar pattern of
381 periods of elevated displacements can be seen.

382 On 17 July 2009, a prolonged period of elevated microseismic activity was observed, with
383 peak displacement amplitudes reaching maxima of ~12 μm and ~16 μm in the n and e
384 directions respectively, though elevated ground displacements above 'background' levels in
385 the z direction are less pronounced. In November/December 2009, a similar prolonged and
386 high amplitude episode of displacement occurred between 29 and 30 November. Again, this
387 is mostly apparent in the n and e directions, which displayed peak amplitudes of ~10 μm but
388 also shorter-lived peak displacements of ~15 μm. Further elevated, yet less sustained, ground
389 displacements occurred on 6 December 2009.

390 A thorough analysis of environmental controls on microseismic displacement is beyond the
391 scope of this paper (see Norman, 2012; and Normal et al., in revision). However, qualitative
392 comparison of environmental and microseismic datasets (Fig. 3) suggests that the majority of
393 the elevated amplitude ground displacements results from a critical combination of key
394 prevailing meteorological, tidal and oceanographic conditions that are typical of infrequent
395 storm events. These events are characterised by reduced atmospheric pressure, increased

396 rainfall, high velocity onshore winds, high tidal residuals and elevated significant wave
397 heights (Fig. 3).

398 3.3.2 Characteristic displacement scenarios

399 To consider variations in microseismic displacement more fully, periods during which
400 particular environmental conditions prevail (i.e. 'displacement scenarios') are now examined.
401 For both datasets (July and November/December 2009) we consider examples of
402 displacement during both low and high tide conditions during a neap tidal phase (LT_{neap} and
403 HT_{neap} respectively), and during low and high tide conditions during a spring tidal phase
404 (LT_{spring} and HT_{spring} respectively). In addition the effects of storm conditions during the
405 November/December 2009 period are examined (Fig. 3 b) during both low and high tide
406 conditions (LT_{storm} and HT_{storm} respectively), and in July 2009 (Fig. 3 a) during high tide
407 conditions (HT_{storm}). Given the semidiurnal tidal cycle, we define the duration of each
408 displacement scenario as a three-hour time window (i.e. 1.08×10^6 observations) centred on
409 the tidal maxima (high tide) or minima (low tide). These time periods selected are shown in
410 Fig. 3.

411 3.3.3 Displacement magnitude

412 Since displacement and strain are related to stress change (Equation 1), we firstly
413 demonstrate the relative frequency of displacements across the full spectrum of observed
414 displacement magnitudes during each characteristic scenario. Normalised cumulative
415 frequency plots of displacement for each scenario and for each component of ground motion
416 (z, n and e) are displayed in Fig. 4.
417

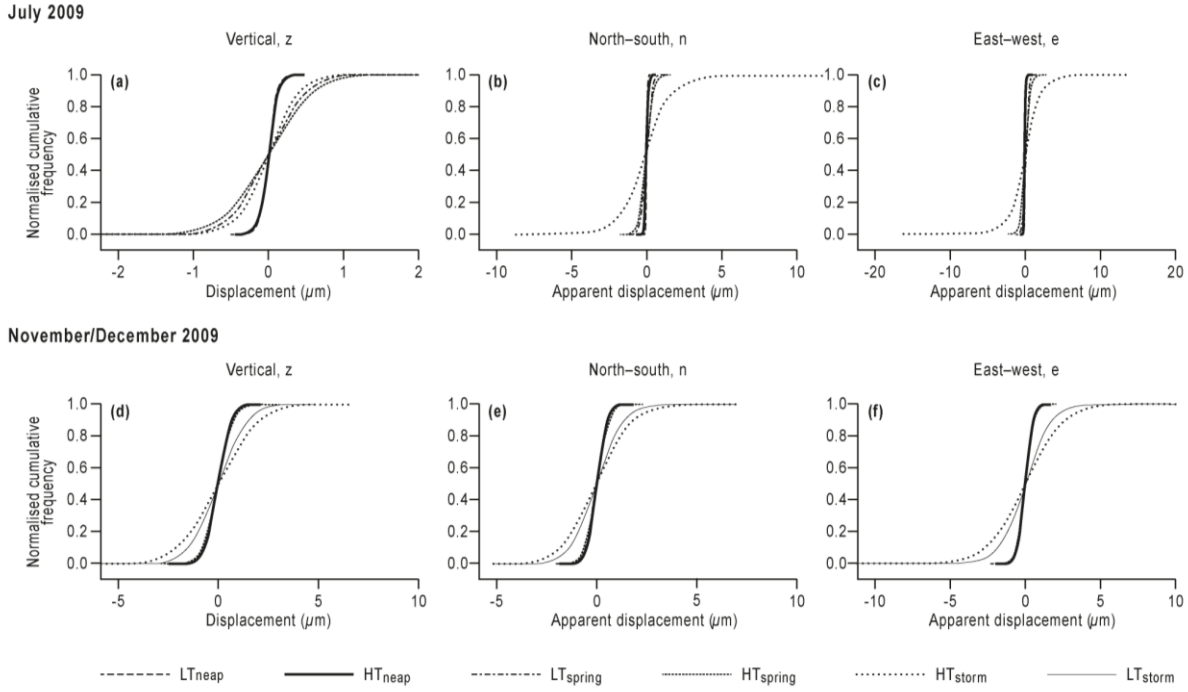

418

419 Fig. 4. Normalised cumulative frequency plots of displacement for July 2009 (a – c) and
420 November-December 2009 (d – f). See main text for an explanation of notation.

Tidal control on displacement amplitude is apparent but is less pronounced than in previously published studies (cf. Adams et al., 2005). In July 2009, the standard deviation of displacement ranges from ~0.1 μm (neap tides) to ~0.5 μm (spring tides) in the z, n and e components. The maximum peak displacement amplitudes observed during neap and spring conditions in the absence of storm events are ~0.3 – 3.0 μm. In November/December 2009, the standard deviation of displacement ranges from ~0.4 μm (neap tides) to ~0.6 μm (spring tides) in the z, n and e components. The maximum peak displacements amplitudes observed range from ~1.5 – 3.0 μm in the z, n and e components.

The control of storm events in generating greater displacement amplitudes is apparent in both the n and e components during both high and low tide conditions. During HT_{storm} in both July 2009 and November 2009, standard deviations of peak displacement amplitude reached ~2 μm in both the n and e components. Some tidal control on displacement during storms is apparent in November 2009; standard deviations of displacement amplitude are lower during LT_{storm} (n component: 1.1 μm; e component: 1.5 μm) than during HT_{storm} conditions (n component: 1.5 μm; e component: 2.1 μm).

Very infrequently occurring ($p < 0.0001$) peak displacement amplitudes observed during 'storm' conditions are an order of magnitude greater than those observed under non-storm conditions, reaching ~16 μm in the e component in July 2009 (HT_{storm}) and ~11 μm in the e component in November 2009. The effect of storm events on displacement in the z direction is less pronounced within the frequency band considered.

3.3.4 Displacement direction

Since the direction of displacement and, hence, stress application may be of significance for fatigue crack growth (Section 2.4), it is important to consider the directional component of

444 microseismic motion for each of the displacement scenarios. For exemplary purposes, we
445 consider the horizontal component of ground motion only. Principal Component Analysis
446 was undertaken on successive groups of 350 observations (i.e. 3.5 s of data per group, a
447 duration equal to the modal wave period observed offshore; Section 3.1). For each 3.5 s
448 group, the resultant azimuth of horizontal ground motion was calculated. Histograms of the
449 frequency distribution of the azimuth of horizontal ground motion for each characteristic
450 displacement scenario are given in Fig. 5.

451 In July 2009, horizontal ground displacements displayed little, if any, preferential direction
452 during LT_{neap} and HT_{neap} (Fig. 5). During LT_{spring} and $HT_{spring,}$ ground displacement frequency
453 distributions display bimodality, with peaks at c. 60°/240° and 150°/330°, though the latter is
454 less pronounced for HT_{spring}. During HT_{storm} for July 2009, modal peaks in ground
455 displacement frequency exist at 45°/225° and, most clearly, at 110°/290°, which is
456 approximately cliff-parallel. The least frequently observed horizontal ground displacement
457 azimuths occurred between 135°/315° and 165°/345° during HT_{storm} (Fig. 5).

458 Horizontal ground displacements in November/December 2009 also displayed limited
459 obvious preferential motion azimuths during LT_{neap}, HT_{neap}, LT_{neap} and HT_{neap}. In contrast,
460 during LT_{storm} and $HT_{storm,}$ a clear modal peak in ground displacement azimuth exists at
461 ~90°/270°, which again is approximately cliff-parallel (Fig. 5). The least frequently observed
462 horizontal ground displacement azimuths occurred broadly in the north-south direction
463 (approximately cliff-normal) during LT_{storm} and HT_{storm} (Fig. 5).
464

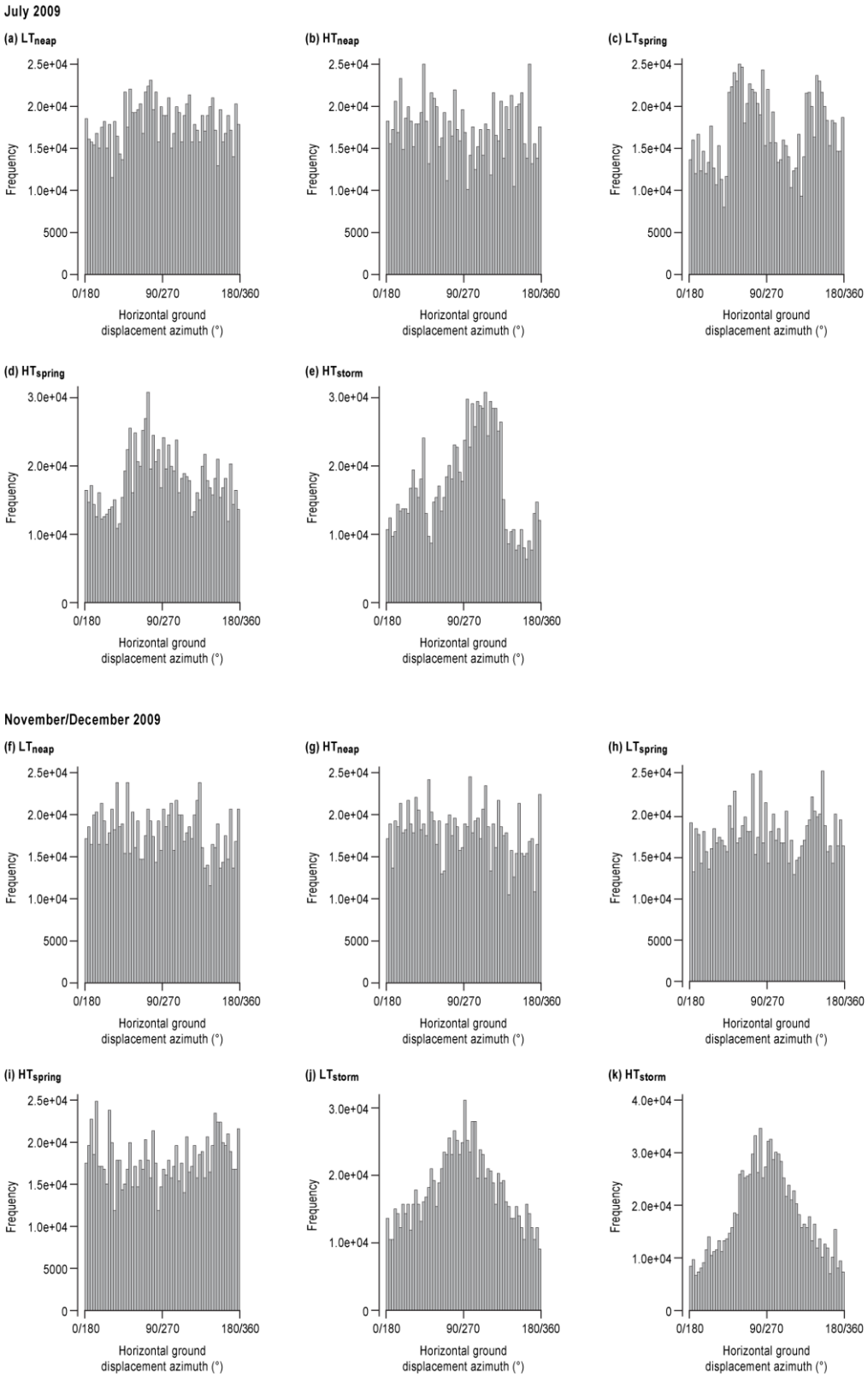

Fig. 5. Frequency distributions of azimuth of horizontal ground displacement for characteristic displacement scenarios for July 2009 (a to e) November-December 2009 (f to k). See main text for an explanation of notation.

Implications

3.3.5 Variable stress amplitude loading

Our data suggest that coastal rock cliffs are subjected to varying cyclic stress amplitudes. Since conventional S-N curves are developed using constant amplitude loading, they are not appropriate in assessing rates of damage accumulation in this setting. Conventional fracture mechanics suggests that varying microseismic displacement amplitudes will profoundly affect the rate of fatigue-driven crack growth following crack initiation, and only if dynamic stress amplitudes are sufficient. The greater cyclic stress amplitudes that occur during storm events will result in a greater change in the crack tip intensity, K (Equation 2). This opens the crack beyond that resulting from background cyclic loads, but also creates a large plastic damage zone around the crack tip (Faulkner et al., 2011), and potentially blunting the crack tip (Suresh, 1998; Petley and Petley, 2006). This results in a localised stress drop as local peak strength is exceeded (cf. Mitchell and Faulkner, 2008) and a less severe stress concentration than that at a sharp crack tip (Suresh, 1998).

During non-storm conditions, the more frequent lower amplitude cyclic stresses may cause the microcrack to grow into the plastic zone created during ‘storm’ loading, resulting in a short-lived increase in the rate of microcrack growth. However, high residual compressive stresses now exist within the plastic zone due to the surrounding elastically stressed material that is yet to fail (Janssen et al., 2002). Residual deformation is created in the areas previously occupied by the crack tip plastic zone, causing microcrack closure (Janssen et al., 2002). Together, these effects may in theory result in a significantly reduced rate, or indeed a cessation, of crack growth that persists until the microseismic stress is increased to a level that is greater than that previously experienced (cf. Lavrov, 2005; Petley et al., 2005 a, b).

493 This ‘additive’ and dynamic threshold is key to defining the location and timing of when
494 microseismic ground motions can be effective.

495 3.3.6 Variability in loading direction

496 The most frequently experienced microseismic loading conditions display a characteristic and
497 limited range of loading directions, with no sustained preferential loading direction. The
498 result is likely to be a constrained stress distribution and plastic zone at the crack tip.
499 Consequently, the rate of crack growth is controlled by the magnitude, frequency and
500 sequencing of displacements, and any resultant thresholds, as defined above. When rare
501 displacement directions, such as those with a greater cliff normal (north-south) component in
502 our study, are experienced, a change to the microscale (crack tip) stress field may result. This
503 may cause greater damage to the rock as the change in loading direction may alter the crack
504 tip separation mode. For example, a Mode I (extension/opening) crack may, under less
505 frequent microseismic loading directions, experience sufficiently significant Mode II (in-
506 plane shear) or Mode III (out-of-plane shear) deformation (Paterson, 1978). Microcracks may
507 as a result switch failure mode or become mixed-mode (Brady and Brown, 2004), promoting
508 growth into previously intact rock, the interaction of otherwise-isolated microcrack
509 populations (cf. Lavrov et al., 2002), and ultimately an increased microcrack density, rock
510 dilatancy and damage (Eberhardt et al., 1999). Changes in loading direction may exploit
511 lithological and structural anisotropy, such as the presence of bedding planes and pre-existing
512 fracture sets that display greater sensitivity to favourably-oriented stress perturbations (cf.
513 Suresh, 1998). The effects of structural anisotropy and variable microscopic failure
514 mechanics are apparent at the both the laboratory (McLamore and Gray, 1967; Niandou et al.,

515 1997; Erarslan and Williams, 2012b) and field scale (Giraud et al., 1990; Agliardi et al.,
516 2001).

517 3.3.7 Episodic damage

518 We surmise that microcrack-driven weakening as a result of microseismic ground
519 displacements may be an highly episodic process. We suggest that microseismic conditions
520 conducive to microcrack propagation, rock damage and a reduction in in peak strength values
521 are only likely to occur extremely rarely, though the frequency of such rare conditions
522 remains difficult to quantify, particularly on the basis of relatively short observational
523 records. These favourable conditions are likely to occur during energetic storm events that
524 infrequently punctuate the lower amplitude microseismic displacements that result from the
525 cyclic ocean wave loading of the foreshore platform. During energetic events (storms),
526 sufficiently high stresses are only generated for a very small fraction of their duration, and
527 indeed are only effective if the previous maximum dynamic stress damage threshold is
528 exceeded. This threshold also depends on the coincidence of two infrequent and apparently
529 independent occurrences: high magnitude displacements (strains) and a rarely-occurring
530 microseismic loading direction (azimuth).

531 Reduced amplitude microseismic ground motions occurring during periods of relative
532 quiescence between storm events may therefore be geomorphologically ineffective, and are
533 physically unable to damage the rock. Curves of strength degradation against time may
534 display stepped rather than continuous reductions in strength that are coincident only with
535 rare displacement conditions during storms (Fig.s 3, 4 and 5). Episodic strength reduction
536 contrasts starkly with the assumptions of the fatigue model proposed by Adams et al. (2005),
537 which suggests that all microseismic displacements cause damage and rock weakening.

Whilst the combination of hydrographic and/or oceanographic controls on the occurrence of episodically damaging microseismic events is likely to be highly site specific, we consider it possible that such episodicity occurs at any site where frequently-experienced microseismic loading conditions are punctuated by 'rare' events that alter the magnitude and nature of ground motion. At our study site, we suggest that such conditions occur during high energy storm events. Elsewhere, such conditions may relate to extreme events that recur over a variety of timescales and result from, for example, regional tectonics and/or the occurrence of tropical storms.

4. Model of microseismic fatigue and damage accumulation

A model is presented to describe our new interpretation of the spatial and temporal pattern of microseismic damage (Fig. 6) with reference to process zones that describe an hypothetical and idealised deviatoric stress distribution within a coastal rock cliff (cf. Wolters and Müller, 2008). We do not explicitly consider the influence of discontinuities within the rock mass. This conceptual model is considered to be applicable to both jointed and homogeneous rock masses in terms of the processes and spatial distribution of microseismic damage. In jointed rock masses, however, we suggest that the processes of fatigue-induced strength degradation may operate along critically-stressed joints and fractures in addition to within the intact rock material (cf. Jafari et al., 2003). We consider three indicative key zones that describe susceptibility to microseismic damage accumulation, but we do not describe the exact form, extent or transition between zones; such characteristics are likely to be gradational and highly site-specific based on, for example, local geological, geomorphological and environmental conditions.

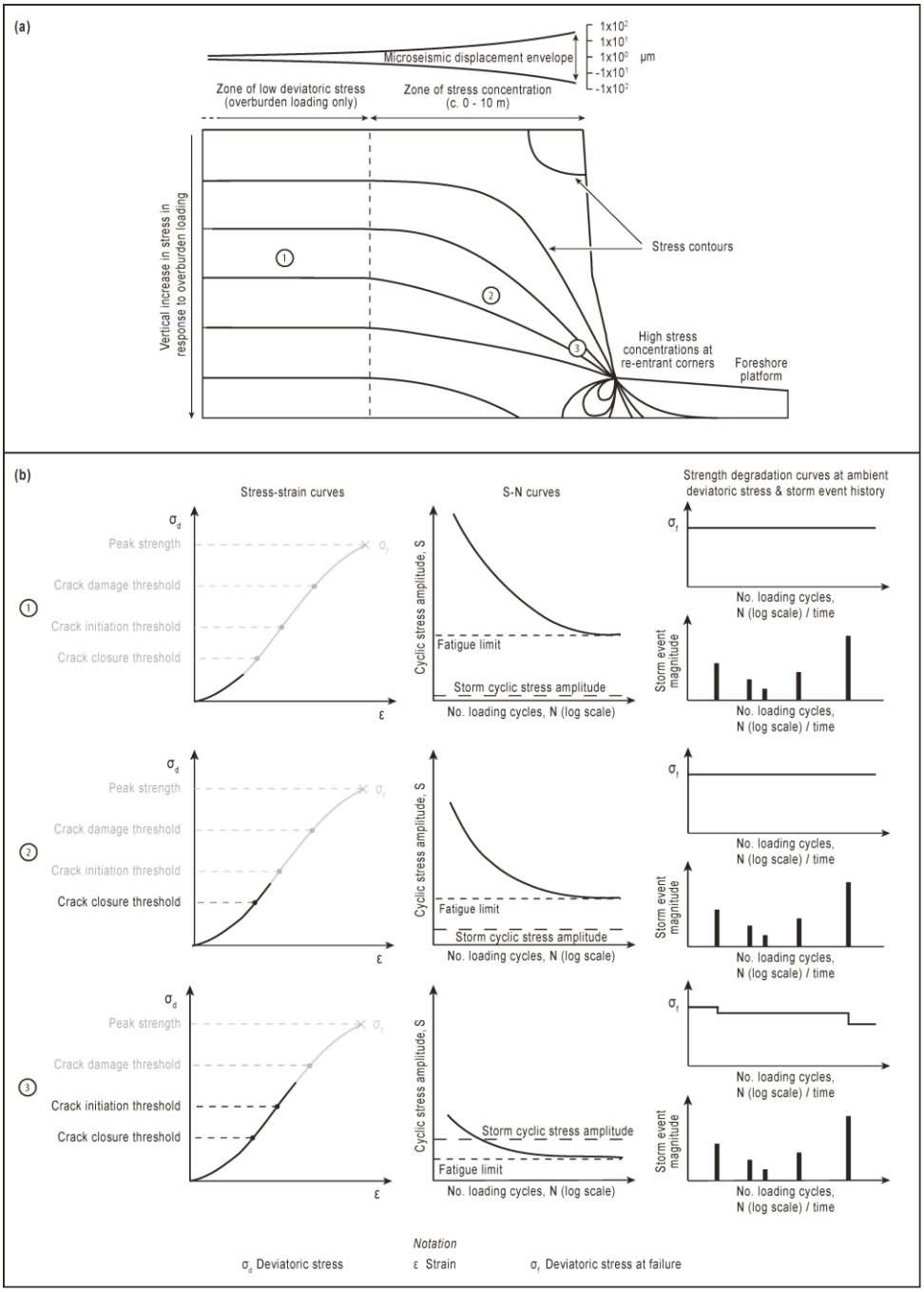

Fig. 6. Conceptual model of the spatial controls on the effectiveness of microseismic damage and the potential episodic evolution of rock mass strength that occurs in response to high energy (storm) loading conditions. (a) Summary of microseismic field conditions detailing patterns of maximum observed microseismic amplitudes, an idealised deviatoric stress distribution and the locations of process zones 1, 2 and 3 (see text for further explanation). (b) Summary of potential stress state and damage conditions in zones 1, 2 and 3 and the potential S-N and strength degradation curves that result from microseismic loading in these zones.

571 Zone 1 is located in the overburden stress loading zone, where deviatoric stresses are low and
572 are insufficient to cause crack closure. Hence, microcrack densities are at background (prior
573 to enhanced 'geomorphic' damage) levels. At this low deviatoric stress level, only a high
574 number of high amplitude cycles operating around the mean stress are capable of causing
575 failure in the rock, as demonstrated by the hypothetical S-N curve. At lower cyclic stress
576 amplitudes, even very high numbers of loading cycles are insufficient to cause
577 microfracturing and fatigue because the rock is insufficiently (pre-)damaged. The rock has a
578 clear fatigue limit because cyclic stress amplitudes caused by microseismic displacement are
579 lower than the fatigue limit. Hence, we suggest that there can be no reduction in strength as a
580 result of microseismic cyclic loading.

581 Zone 2 is located within the zone of stress concentration, where deviatoric stresses begin
582 closure of favourably-oriented microcracks. The rock is in an elastic deformation phase and
583 the rock displays a definite fatigue limit. Despite slightly increased microseismic cyclic stress
584 amplitudes, these are still not greater than the fatigue limit. Hence, there remains no reduction
585 in strength as a result of microseismic cyclic loading.

586 Zone 3 is located within the damage accumulation zone of a pre-formed or incipient fracture
587 resulting from gravitational failure. Here, deviatoric stress is at a level sufficient to initiate
588 microcracking, though ambient static stresses are not sufficient to cause macroscale fracture;
589 crack growth remains subcritical and stable (i.e. less than the crack damage threshold). This
590 increased state of damage renders the rock more susceptible to lower cyclic stress amplitudes.
591 The fatigue limit of the rock may now be less than the cyclic stress amplitudes occurring
592 during storm events, allowing the microseismic displacements to accumulate damage,
593 reducing rock strength such that it is more prone to fracture at lower deviatoric stresses. The

more frequent intervening lower magnitude displacements resulting from foreshore loading by ocean waves, for example, are unlikely to damage the rock due to the effects of crack tip blunting and residual stresses that close microcracks (Section 3.4.1). Although cyclic loading continues during non-storm conditions, we contend that these loading cycles do not damage the rock and there is no corresponding decrease in strength.

Hence, as suggested in the strength degradation curve, reductions in strength resulting from microseismic damage may be episodic, only occurring during high energy conditions that cause the previously experienced maximum dynamic microseismic stress to be exceeded.

5. Discussion

5.1 Geomorphic significance of microseismic ground displacements

By defining the likely spatial extent of damage accumulation zones and through consideration of the relative magnitude-frequency characteristics of microseismic ground displacements resulting from standard tidal loading effects and energetic storm conditions, we suggest that the likely opportunity for cyclic microseismic loading of coastal rock cliffs to cause damage and weakening through propagation and coalescence of microcracks is highly spatially and temporally restricted. Hence, as an isolated process, microseismic displacement may be unlikely to have sufficient opportunity to cause cumulative weakening of rock. This is particularly the case if cliff retreat rates are high relative to the net effect of microseismic damage processes, since a parcel of rock that slowly accumulates microseismic damage is likely to be exhumed, detached or eroded by other more ‘aggressive’ processes before microseismicity exerts a meaningful control on rock strength.

615 In reality, microseismic loading does not operate in isolation. Microseismic damage is part of
616 a range of interacting, environmentally-controlled processes that can potentially effect
617 subcritical crack growth and rock weakening (Pentecost, 1991; Main et al., 1993; Petley et
618 al., 2005 a, b; Gómez-Heras et al., 2006; Hall et al., 2010; Gischig et al., 2011a, b; Smith et
619 al., 2011). These processes act in synergy to increase microcrack density in a subcritical
620 manner before coalescence occurs at a critical level, causing a transition from secondary to
621 tertiary creep and, hence, an acceleration in crack growth rate that is no longer controlled by
622 environmental forcing (Rosser et al., 2007). Microseismic ground displacements may only
623 operate as an effective geomorphic agent, particularly as a preparatory weakening process (cf.
624 Adams et al., 2005), as part of this suite of complementary processes.

625 5.2 Magnitude-frequency distribution of microseismic events

626 Our hypothesis that microseismic contributions to damage accumulation are episodic has
627 significant implications for our understanding of the environmental controls on microseismic
628 damage. We contend that environmental processes that cause greater displacements (such as
629 storms) than those during standard loading conditions may result in solely tidally-controlled
630 displacements being ineffective. Damage is contingent upon both the magnitude-frequency
631 distribution of displacement and not solely magnitude alone. Consequently, inter-site
632 comparison of displacement amplitudes in terms of damage and fatigue effects is unlikely to
633 be meaningful without a full understanding of the full microseismic displacement and
634 direction magnitude-frequency distributions at each site. This has important implications for
635 the microseismic monitoring period itself; shorter duration monitoring periods lasting a few
636 weeks, months or even years, are unlikely to capture the most damaging microseismic
637 consequences. We advocate significantly longer monitoring campaigns tailored to the

638 recurrence of extremes (cf. Norman, 2012) to capture as much of the magnitude-frequency
639 distribution and to better define what constitutes infrequent, highly damaging microseismic
640 conditions.

641 5.3 Constraining the influence of microseismic damage on rockfall occurrence

642 Comparison of environmental (meteorological and oceanographic) processes with rockfall
643 inventories at our study site has revealed few strong, statistically significant correlations
644 (Rosser et al., 2007; Lim et al., 2010). This may result from the highly spatially specific and
645 temporally restricted nature of microseismic damage potential and the temporal nature of
646 fatigue microcrack growth.

647 Typically, attempts to correlate environmental processes with rockfall activity (the ultimate
648 results of damage accumulation) are undertaken at relatively coarse temporal resolution
649 (monthly, for example; cf. Rosser et al., 2007). Rock-damaging microseismic conditions
650 (suitably-coincident magnitude and direction of displacement) occur infrequently but rapidly
651 (over seconds) and at the microscale. Hence, comparison of time-averaged microseismic
652 displacement data recorded at the cliff top with regional scale and time-averaged (hourly)
653 oceanographic and/or meteorological datasets is unlikely to reveal the exact combination of
654 environmental conditions required to cause microseismic damage. Greater temporal and
655 spatial resolution of data describing environmental conditions may help to improve this
656 linkage.

657 During the most damaging microseismic conditions (storms, for example), it is also likely
658 that other processes conducive to damage and subsequent fracture, such as pore water
659 pressure increases (Brooks et al., 2012), or ocean wave impact loading at the cliff base
660 (Kirkgöz, 1990), also increase in magnitude and potential geomorphic effectiveness. Hence,

isolating the damage effect of each forcing variable becomes extremely difficult if not impossible in the field. This may further obscure any direct relationships between the development of fractures, manifest as rockfall activity, and microseismic loading.

Finally, if microcrack densities have evolved to a critical level, then a sufficiently large microseismic displacement episode may act as a catalyst for failure as critical strain thresholds are exceeded (Petley et al, 2005 a, b). Such an event is also not likely to be easily isolated or detected as the direct trigger mechanism of subsequent macro-scale fracture and rockfall activity, which requires an 'internal' self-organising yet highly time-dependent cascade of microcrack development and coalescence (Main et al., 1993). This process temporally separates cause from effect. The phenomenon of failure with no apparent direct environmental trigger has previously been recognised in monitoring datasets in coastal rock cliff environments (Rosser et al., 2007). Indeed, the microscale mechanical cracking processes that we propose conforms to the damage accumulation model developed by Rosser et al. (2007), which is based on temporal patterns of strain accumulation and rockfall within brittle coastal rock cliff materials.

6. Conclusions

By drawing together appropriate literature, theory and field data, we have reassessed the potential role that microseismic ground displacements may play in propagating microfractures and subsequently weakening rock masses via a cyclic loading and fatigue process. Our conclusions are:

1. Due to the low magnitude of the strains and resultant stresses generated, microseismic ground motions are likely to require rocks to undergo a critical level of stress and strain (i.e. a pre-damaged condition) before they can drive microcrack damage and fatigue. It is

suggested that such critical stressing occurs only in ‘damage accumulation zones’ of limited spatial extent, as governed by macroscale stress states, here shown in the near-cliff face stress concentration.

2. Microseismic ground displacements observed at our study site demonstrate low background amplitudes that display limited response to tide level. This relative quiescence in microseismic ground motion is interrupted by periods of greater displacement during energetic storm events. Higher amplitude displacements extend microcracks beyond conditions achievable by low amplitude background displacements, but by doing so cause blunting of microcrack tips and generate local residual stresses, which close the microcrack and curtail microcrack growth. The intervening and ongoing cyclic loading that occurs during non-storm events may therefore be insufficient to damage and weaken the rock mass.
3. At times of greatest displacement amplitude, our analysis demonstrates less frequent ground motions with a strong cliff normal component. These rarer displacements are likely to be more damaging, as they may cause a change in the microcrack tip stress distribution and separation mode and/or may cause interaction of microcrack populations that would not normally interact under standard (‘background’) loading conditions.
4. In response to the low frequency of occurrence of microseismic events that may damage rock, microseismic damage and strength degradation may occur episodically, rather than continuously in (quasi-)proportional and cumulative response to environmental forcing.
5. The necessary conditions for damage are highly restrictive, both spatially and temporally. Hence, we hypothesise that there is unlikely to be sufficient opportunity for microseismic ground motions to cause geomorphologically significant rock weakening, particularly when considered in the context of other processes in action. Whilst microseismic

displacements may, under suitable conditions, trigger changes in the rate of microcrack growth, elucidating the relationship between microseismic cause and rockfall effect is not straightforward.

Acknowledgements

This work was funded and supported by Cleveland Potash Ltd., which we gratefully acknowledge. We are also very grateful to the following: SEIS-UK for use of the microseismoters (NERC GEF loan 879) and for technical support and field assistance; NERC BIGF for GPS data; NERC BODC for oceanographic data; Peter Adams and Dave Milledge for sharing and discussing seismic data processing code; Chris Orton for assistance with drafting figures; Mike Lim and Sam Waugh for help during the fieldwork phase; Antony Long for helpful comments on an earlier draft of the manuscript; and Alex Densmore for useful discussions. We thank Adam Young and Mark Dickson for their detailed reviews of the manuscript and their helpful comments.

References

Adams, P. N., Anderson, R.S. and Revenaugh, J., 2002, Microseismic measurement of wave-energy delivery to a rocky coast. Geology, 30: 895-898.

Adams, P.N., Storlazzi, C.D. and Anderson, R.S., 2005. Nearshore wave-induced cyclical flexing of sea cliffs. Journal of Geophysical Research, 110, F02002. doi:10.1029/2004JF000217

Agar, R., 1960. Post–glacial erosion of the North Yorkshire Coast from the Tees Estuary to Ravenscar. Proceedings of the Yorkshire Geological Society, 32: 409–428.

729 Agliardi, F., Crosta, G. and Zanchi, A., 2001. Structural constraints on deep-seated slope
730 deformation kinematics. Engineering Geology, 59: 83 – 102.

731 Allison, R.J., 1996. Stress and strain in geomorphology. In Mäusbacher, R. and Schulte, A.
732 (eds). Readings in Physical Geography. Springer-Verlag, Heidelberg.

733 Anders, M. H. and Wiltschko, D.V., 1994. Microfracturing, paleostress and the growth of
734 faults. Journal of Structural Geology, 16: 795–815.

735 Attewell, P.B. and Farmer, I.W., 1973.Fatigue behaviour of rock. International Journal of
736 Rock Mechanics and Mining Sciences, 10: 1 – 9.

737 Barlow, J., Lim, M., Rosser, N., Petley, D. Brain, M., Norman, E. and Geer, M., 2012.
738 Modeling cliff erosion using negative power law scaling of rockfalls. Geomorphology 139 –
739 140: 416 – 424. doi:10.1016/j.geomorph.2011.11.006

740 Bieniawski, Z.T., 1967. Mechanism of brittle rock fracture. Part I: theory of the fracture
741 process. International Journal of Rock Mechanics and Mining Sciences and Geomechanics
742 Abstracts, 4: 395-406.

743 Bjerrum, L., 1967, Progressive failure in slopes of overconsolidated plastic clay and clay
744 shales. Journal of the Soil Mechanics and Foundations Division of the American Society of
745 Civil Engineers, 93: 1–49.

746 Brace, W.F., Paulding Jr., B.W. and Scholz, C., 1966. Dilatancy in the fracture of crystalline
747 rocks. Journal of Geophysical Research, 71: 3939 – 3953. doi:10.1029/JZ071i016p03939

748 Brady, B.H.G. and Brown, E.T. 2004. Rock Mechanics for Underground Mining. Klewer
749 Academic Publishers, Dordrecht.

750 Brooks, S.M., Spencer, T. and Boreham, S., 2012. Deriving mechanisms and thresholds for
751 cliff retreat in soft-rock cliffs under changing climates: Rapidly retreating cliffs of the Suffolk
752 coast, UK. Geomorphology, 153 – 154: 48 – 60.

753 Cai, M., Kaiser, P.K., Tasaka, Y., Maejima, T., Morioka, H. and Minami, M., 2004.
754 Generalized crack initiation and crack damage stress thresholds of brittle rock masses near
755 underground excavations. International Journal of Rock Mechanics & Mining Sciences, 41:
756 833 – 847.

757 Clarke, B.A. and Burbank, D.W., 2010. Bedrock fracturing, threshold hillslopes, and limits to
758 the magnitude of bedrock landslides. Earth and Planetary Science Letters, 297, 577 – 586.
759 doi:10.1016/j.epsl.2010.07.011

760 Clarke, B.A. and Burbank, D.W., 2011. Quantifying bedrock-fracture patterns within the
761 shallow subsurface: Implications for rock mass strength, bedrock landslides, and erodibility.
762 Journal of Geophysical Research, 116, F04009. doi: 10.1029/2011JF001987

763 Crawford, W. C., and Webb, S.C., 2000. Identifying and removing tilt noise from low-
764 frequency (<0.1 Hz) seafloor vertical seismic data, Bulletin of the Seismological Society of
765 America, 90: 952 – 963. doi: 10.1785/0119990121.

766 Dammeier, F., Moore, J.R., Haslinger, F. and Loew S., 2011.Characterization of alpine
767 rockslides using statistical analysis of seismic signals. Journal of Geophysical Research, 116,
768 F04024. doi:10.1029/2011JF002037

769 Deparis, J., Jongmans, D., Cotton, F., Baillet, L., Thouvenot, F. And Hantz, D., 2008.
770 Analysis of Rock-Fall and Rock-Fall Avalanche Seismogramsin the French Alps. Bulletin of
771 the Seismological Society of America, 98: 1781 – 1796. doi: 10.1785/0120070082

772 Dickson, M.E. and Pentney, R., 2012. Micro-seismic measurements of cliff motion under
773 wave impact and implications for the development of near-horizontal shore platforms.
774 Geomorphology 151 – 152: 27 – 38. doi:10.1016/j.geomorph.2012.01.006

775 Dühnforth, M., Anderson, R.S., Ward, D and, Stock, G.M., 2010. Bedrock fracture control of
776 glacial erosion processes and rates. Geology, 38, 423 – 426. doi: 10.1130/G30576.1

777 Eberhardt, E., Stead, D. and Stimpson, B., 1999. Quantifying progressive pre-peak brittle
778 fracture damage in rock during uniaxial compression. International Journal of Rock
779 Mechanics and Mining Sciences, 36: 361 – 380.

780 Eberhardt, E. Stead, D. and Coggan, J.S., 2004. Numerical analysis of initiation and
781 progressive failure in natural slopes – the 1991 Randa rockslide. International Journal of
782 Rock Mechanics and Mining Sciences, 41: 69 – 87.

783 Erarslan, N. and Williams, D.J., 2012a. Investigating the effect of cyclic loading on the
784 indirect tensile strength of rocks. Rock Mechanics and Rock Engineering, 45: 327 – 340. doi:
785 10.1007/s00603-011-0209-7

786 Erarslan, N. and Williams, D.J., 2012b. Mechanism of rock fatigue damage in terms of
787 fracturing modes. International Journal of Fatigue, 43: 76 – 89.
788 doi:10.1016/j.ijfatigue.2012.02.008

789 Faulkner, D.R., Mitchell, T.M., Healy, D. and Heap, M.J., 2006. Slip on 'weak' faults by the
790 rotation of regional stress in the fracture damage zone. Nature, 444: 922-
791 955.doi:10.1038/nature05353

792 Faulkner, D.R., Mitchell, T.M., Jensen, E., and Cembrano, J. 2011. Scaling of fault damage
793 zones with displacement and the implications for fault growth processes. Journal of
794 Geophysical Research, 116, B05403. doi:10.1029/2010JB007788

795 Giraud, A., Rochet, L. And Antoine, P., 1990. Processes of slope failure in crystallophyllian
796 formations. Engineering Geology, 29: 241 – 253.

797 Gischig, V.S., Moore, J.R., Evans, K.F., Amann, F. and Loew, S., 2011a. Thermomechanical
798 forcing of deep rock slope deformation: 1. Conceptual study of a simplified slope. Journal of
799 Geophysical Research, 116, F04010. doi:10.1029/2011JF002006

800 Gischig, V.S., Moore, J.R., Evans, K.F., Amann, F. and Loew, S., 2011b. Thermomechanical
801 forcing of deep rock slope deformation: 2. The Randa rock slope instability. Journal of
802 Geophysical Research, 116, F04011. doi:10.1029/2011JF002007

803 Gómez-Heras, M., Smith, B.J. and Fort, R., 2006. Surface temperature differences between
804 minerals in crystalline rocks: Implications for granular disaggregation of granites through
805 thermal fatigue. Geomorphology, 78: 236 - 249.

806 Graizer, V., 2006. Tilts in strong ground motion, Bulletin of the Seismological Society of
807 America, 96: 2090–2102. doi:10.1785/0120060065.

808 Gunzberger, Y., Merrien-Soukatchoff, V. and Guglielmi, Y., 2005. Influence of daily surface
809 temperature fluctuations on rock slope stability: case study of the Rochers de Valabres slope

(France). International Journal of Rock Mechanics and Mining Sciences, 42: 331 – 349. doi:10.1016/j.ijrmms.2004.11.003

Hall, C., Hamilton, A., Woff, W.D., Viles, H.A. and Eklund, J.A., 2011. Moisture dynamics in walls: response to micro-environment and climate change. Proceedings of the Royal Society A, 467: 194-211 doi: 10.1098/rspa.20100131.

Heap, M.J., Baud, P. and Meredith, P.G., 2009. The influence of temperature on brittle creep in sandstones. Geophysical Research Letters, 36, L19305.doi:10.1029/2009GL039373

Heap, M.J., Faulkner, D.R., Meredith, P.G. and Vinciguerra, S., 2010. Elastic moduli evolution and accompanying stress changes with increasing crack damage: implications for stress changes around fault zones and volcanoes during deformation. Geophysical Journal International, 183: 225 – 236. doi: 10.1111/j.1365-246X.2010.04726.x

Hobbs, D.W., 1964. The tensile strength of rocks. International Journal of Rock Mechanics and Mining Sciences, 1: 385 – 396.

Hoek E. and Bieniawski Z.T., 1965. Brittle fracture propagation in rock under compression. International Journal of Fracture Mechanics, 1: 137 – 155.

Hsu, L., Finnegan, N.J. and Brodsky, E.E., 2011. A seismic signature of river bedload transport during storm events. Geophysical Research Letters, 38, L13407. doi:10.1029/2011GL047759, 2011

Jafari, M.K., Amini Hosseini, K., Pellet, F., Boulon, M. and Buzzi, O., 2003. Evaluation of shear strength of rock joints subjected to cyclic loading. Soil Dynamics and Earthquake Engineering, 23: 619 – 630.

831 Janssen, C., Wagner, F.C., Zang, A. and Dresen, G., 2001. Fracture process zone in granite:
832 a microstructural analysis. International Journal of Earth Sciences, 90: 46–59.
833 doi:10.1007/s005310000157

834 Janssen, M., Zuidema, J. and Wanhill, R. 2002. Fracture Mechanics. Spon Press/Taylor and
835 Francis Group, London/New York.

836 Kirkgöz, M.S. 1990. An experimental investigation of a vertical wall response to breaking
837 wave impact. Ocean Engineering, 17: 379 – 391.

838 Koons, P.O., Upton, P. and Barker, A.D. 2012. The influence of mechanical properties on the
839 link between tectonic and topographic evolution. Geomorphology, 137 (1), 168 – 180.
840 doi:10.1016/j.geomorph.2010.11.012

841 Kranz, R.L., 1983. Microcracks in rocks: a review. Tectonophysics, 100: 449 – 480.

842 Lajtai, E.Z., 1971. A theoretical and experimental evaluation of the Griffth theory of brittle
843 fracture. Tectonophysics, 11:129 - 156.

844 Lavrov, A., Vervoort, A., Wevers, M., Napier, and Napier, J.A.L., 2002. Experimental and
845 numerical study of the Kaiser effect in cyclic Brazilian tests with disk rotation. International
846 Journal of Rock Mechanics and Mining Sciences, 39: 287 – 302.

847 Li, G., Moelle K.H. and Lewis, J.A., 1992. Fatigue crack growth in brittle Sandstones.
848 International Journal of Rock Mechanics and Mining Sciences and Geomechanics Abstracts,
849 2: 469 – 77.

Lim, M., Rosser, N., Allison, R. & Petley, D. 2010a. Erosional processes in the hard rock coastal cliffs at Staithes, North Yorkshire. Geomorphology, 114: 12 - 21. doi:10.1016/j.geomorph.2009.02.011

Lim, M., Rosser, N.J., Petley, D.N. and Keene, M, 2011. Quantifying the Controls and Influence of Tide and Wave Impacts on Coastal Rock Cliff Erosion. Journal of Coastal Research, 27: 46-56. doi:10.2112/JCOASTRES-D-09-00061.1

McLamore, R. and Gray, K.W., 1967.The mechanical behaviour of anisotropic sedimentary rocks. Journal of Engineering for Industry, Transactions of the American Society of Mechanical Engineers, Series B, 89: 62 – 76.

Main, I.G., Sammonds, P.R. and Meredith, P.G., 1993. Application of a modified Griffith criterion to the evolution of fractal damage during compressional rock failure. Geophysical Journal International, 115: 367–380. doi: 10.1111/j.1365-246X.1993.tb01192.x

Martin, C.D. and Chandler, N.A., 1994. The progressive fracture of Lac du Bonnet granite. International Journal of Rock Mechanics and Mining Sciences and Geomechanics Abstracts, 31: 643 – 659.

Mitchell, T.M. and Faulkner, D.R., 2008. Experimental measurements of permeability evolution during triaxial compression of initially intact crystalline rocks and implications for fluid flow in fault zones. Journal of Geophysical Research, 113, B11412. doi:10.1029/2008JB005588, 2008

Molnar, P., Anderson, R.S. and Anderson, S.P., 2007. Tectonics, fracturing of rock, and erosion. Journal of Geophysical Research, 112, F03014. doi:10.1029/02005JF000433.

871 Moore, D. E. and Lockner, D.A., 1995. The role of microcracking in shear-fracture
872 propagation in granite. Journal of Structural Geology, 17: 95 – 114.

873 Moore, J.R., Sanders, J.W., Dietrich, W.E. and Glaser, S.D., 2009. Influence of rock mass
874 strength on the erosion rate of alpine cliffs. Earth Surface Processes and Landforms, 34: 1339
875 – 1352. doi: 10.1002/esp.1821

876 Nasseri, M.H.B., Grasselli, G. and Mohanty, B. 2010. Fracture Toughness and Fracture
877 Roughness in Anisotropic Granitic Rocks. Rock Mechanics and Rock Engineering, 43: 403 –
878 415. doi: 10.1007/s00603-009-0071-z

879 Ng, K-Y. And Petley, D.N., 2009. The use of pore pressure reinflation testing in landslide
880 management in Hong Kong. Quarterly Journal of Engineering Geology and Hydrogeology,
881 42: 487 - 498.

882 Niandou, H., Shao, J.F., Henry, J.P. and Fourmaintraux, D., 1997. Laboratory investigation of
883 the mechanical behaviour of Tournemore Shale. International Journal of Rock Mechanics
884 and Mining Sciences, 34: 3 – 16.

885 Norman, E.C. 2012. Microseismic monitoring of the controls on coastal rock cliff erosion.
886 Unpublished PhD thesis, Durham University, UK. http://etheses.dur.ac.uk/3586/

887 Norman, E.C., Rosser, N.J., Brain, M.J., Petley, D.N. and Lim, M. In revision. Coastal cliff-
888 top ground motions as proxies for environmental processes. Journal of Geophysical Research
889 – Oceans.

890 Paterson, M.S., 1978. Experimental Rock Deformation – the Brittle Field. Springer, Berlin.

891 Peng, S. and Johnson, A.M., 1972. Crack growth and faulting in cylindrical specimens of
892 Chelmsford granite. International Journal of Rock Mechanics and Mining Sciences and
893 Geomechanics Abstracts, 9: 37 – 86.

894 Pentecost, A., 1991. The weathering rates of some sandstone cliffs, Central Weald, England.
895 Earth Surface Processes and Landforms, 16: 83 - 91.

896 Petley, D.N., Higuchi, T., Petley, D.J., Bulmer, M.H. and Carey, J., 2005a. Development of
897 progressive landslide failure in cohesive materials. Geology, 33: 201 – 204. doi:
898 10.1130/G21147.1

899 Petley, D.N., Higuchi, T., Dunning, S., Rosser, N.J., Petley, D.J., Bulmer, M.H.K. and Carey,
900 J.2005b. A new model for the development of movement in progressive landslides. In:
901 Hungr, O., Fell, R., Couture, R. & Eberhardt, E. Landslide Risk Management. Balkema,
902 Amsterdam.

903 Petley, D. N. & Petley, D. J., 2006. On the initiation of large rockslides: perspectives from a
904 new analysis on the Vaiont movement record. In: Mugnozza, G., Strom, A. & Hermanns, R.
905 L. (eds). Massive Rock Slope Failure. NATO. Rotterdam.

906 Potyondy, D.O., 2007. Simulating stress corrosion with a bonded-particle model for rock.
907 International Journal of Rock Mechanics and Mining Sciences, 44: 677 – 691.
908 doi:10.1016/j.ijrmms.2006.10.002

909 Rawson, P.F. and Wright, J.K., 2000. The Yorkshire Coast. The Yorkshire Coast Geologists'
910 Association Guide No. 34. Geologists' Association, London.

911 Robinson, L.A. 1974. Towards a process response model of cliff retreat—the case of North
912 East Yorkshire. Unpublished PhD thesis, University of Leeds, UK.

913 Rodgers, P. W., 1968. Response of horizontal pendulum seismometer to Rayleigh and love
914 waves tilt and free oscillations of Earth. Bulletin of the Seismological Society of America,
915 58: 1384 – 1406.
916
917 Rosser, N.J., Lim, M., Petley, D.N. and Dunning, S.A. 2007. Patterns of precursory rockfall
918 prior to slope failure. Journal of Geophysical Research, 112, F04014.
919 doi:10.1029/2006JF000642.

920 Roux. P-F, Marsan, D., Métaxian, J-P, O'Brien, G. and Moreau, L. 2008. Microseismic
921 activity within a serac zone in an alpine glacier (Glacier d'Argentière, Mont Blanc, France).
922 Journal of Glaciology, 54: 157 – 168. doi:10.3189/002214308784409053

923 Scholz, C.H., 1968. Microfracturing and inelastic deformation of rock in compression.
924 Journal of Geophysical Research, 73: 1417 – 1432.

925 Smith, B.J., McCabe, S., McAllister, D., Adamson, C., Viles, H.A. and Curran, J.M., 2011. A
926 commentary on climate change, stone decay dynamics and the 'greening' of natural stone
927 buildings: new perspectives on 'deep wetting'. Environmental Earth Sciences, 63:1691–1700.
928 Doi: 10.1007/s12665-010-0766-1

929 Stock, G.M., Martel, S.J., Collins, B.D. and Harp, E.L. 2011. Progressive failure of sheeted
930 rock slopes: the 2009–2010 Rhombus Wall rock falls in Yosemite Valley, California, USA.
931 Earth Surface Processes and Landforms, 37, 546 – 561. doi: 10.1002/esp.3192

932 Styles, T.D., Coggan, J.S. and Pine, R.J., 2011. Back analysis of the Joss Bay Chalk Cliff
933 Failure using numerical modelling. Engineering Geology, 120: 81 – 90.
934 doi:10.1016/j.enggeo.2011.04.004

935 Sunamura, T. 1992. Geomorphology of Rocky Coasts. John Wiley and Sons, Chichester.

936 Suresh, S., 1998. Fatigue of Materials. Cambridge University Press, Cambridge.

937 Tapponier, P. and Brace, W.F., 1976. Development of stress-induced microcracks in
938 Westerly Granite. International Journal of Rock Mechanics and Mining Sciences and
939 Geomechanics Abstracts, 13: 103 – 112.

940 Terzaghi, K., 1962. Stability of steep slopes on hard unweathered rock. Géotechnique, 12:
941 251 – 270.

942 Tien Y.M., Lee D.H. and Juang C.H., 1990. Strain, pore pressure and fatigue characteristics
943 of sandstone under various load conditions. International Journal of Rock Mechanics and
944 Mining Sciences and Geomechanics Abstracts, 27, 283 – 289.

945 Tsai, V.C., Minchew, B., Lamb, M.P. and Ampuero, J-P., 2012. A physical model for seismic
946 noise generation from sediment transport in rivers. Geophysical Research Letters, 39,
947 L02404. doi:10.1029/2011GL050255

948 Vermilye, J. M. and Scholz, C.H., 1998. The process zone: A microstructural view of fault
949 growth, Journal of Geophysical Research, 103: 12,223–12,237.

950 Vinciguerra, S., Trovato, C., Meredith, P.G. and Benson, P.M., 2005. Relating seismic
951 velocities, thermal cracking and permeability in Mt. Etna and Iceland basalts, International
952 Journal of Rock Mechanics and Mining Sciences, 42: 900 – 910.

953 Webb, S. C., and Crawford, W.C., 1999. Long-period seafloor seismology and deformation
954 under ocean waves. Bulleting of the Seismological Society of America, 89: 1535 –
955 1542.West, M.E., Larsen, C.F., Truffer, M., O'Neel, S. and LeBlanc, L., 2010. Glacier
956 microseismicity. Geology, 38: 319 – 322. doi: 10.1130/G30606.1

957 Wilson, J. E., Chester, J.S. and Chester, F.M., 2003. Microfracture analysis of fault growth
958 and wear processes, Punchbowl Fault, San Andreas System, California. Journal of Structural
959 Geology, 25: 1855–1873.

960 Wolters, G. and Müller, G., 2008. Effect of cliff shape on internal stresses and rock slope
961 stability. Journal of Coastal Research. 24: 43 – 50. http://dx.doi.org/10.2112/05-0569.1

962 Wyllie, D.C. and Mah, C., 2010. Rock Slope Engineering: Civil and Mining. Spon
963 Press/Taylor and Francis Group, London/New York.

964 Xiao, J-Q, Feng, X-T, Ding, D-X and Jiang, F-L, 2011. Investigation and modeling on fatigue
965 damage evolution of rock as a function of logarithmic cycle. International Journal for
966 Numerical and Analytical Methods in Geomechanics, 35: 1127 – 1140. doi: 10.1002/nag.946

967 Young, A.P. and Ashford, S.A., 2008. Instability investigation of cantilevered seacliffs. Earth
968 Surface Processes and Landforms, 33: 1661 – 1667. doi: 10.1002/esp.1636

969 Young, A.P., Adams, P.N., O'Reilly, W.C., Reinhard, E.F. and Guza, R.T., 2011. Coastal
970 cliff ground motions from local ocean swell and infragravity waves in southern California.
971 Journal of Geophysical Research, 116, C09007. doi:10.1029/2011JC007175

972 Young, A.P., Guza, R.T., Adams, P.N., O'Reilly, W.C. and Flick, R.E. Cross-shore decay of
973 cliff top ground motions driven by local ocean swell and infragravity waves. Journal of
974 Geophysical Research, 117. C06029. doi:10.1029/2012JC007908